

Relativistic outflow in CXO CDFS J033260.0-274748

J. X. Wang^{1,2}, T. G. Wang¹, P. Tozzi³, R. Giacconi², G. Hasinger⁴, L. Kewley⁵, V. Mainieri⁴, M. Nonino³, C. Norman^{2,6}, A. Streblyanska⁴, G. Szokoly⁴, T. Yaqoob^{2,7}, and A. Zirm⁸

ABSTRACT

In this letter we report the detection of a strong and extremely blueshifted X-ray absorption feature in the 1 Ms *Chandra* spectrum of CXO CDFS J033260.0-274748, a quasar at $z = 2.579$ with $L_{2-10\text{keV}} \sim 4 \times 10^{44}$ ergs s⁻¹. The broad absorption feature at ~ 6.3 keV in the observed frame can be fitted either as an absorption edge at 20.9 keV or as a broad absorption line at 22.2 keV rest frame. The absorber has to be extremely ionized with an ionization parameter $\xi \sim 10^4$, and a high column density $N_H > 5 \times 10^{23}$ cm⁻². We reject the possibility of a statistical or instrumental artifact. The most likely interpretation is an extremely blueshifted broad absorption line or absorption edge, due to H or He-like iron in a relativistic jet-like outflow with bulk velocity of $\sim 0.7-0.8c$. Similar relativistic outflows have been reported in the X-ray spectra of several other AGNs in the past few years.

Subject headings: galaxies: active — quasars: individual (CXO CDFS J033260.0-274748) — X-rays: galaxies

¹Center for Astrophysics, University of Science and Technology of China, Hefei, Anhui 230026, P. R. China; jxw@ustc.edu.cn.

²Dept. of Physics and Astronomy, The Johns Hopkins University, Baltimore, MD 21218

³INAF Osservatorio Astronomico, Via G. Tiepolo 11, 34131 Trieste, Italy

⁴Max-Planck-Institut für extraterrestrische Physik, Postfach 1312, D-85741 Garching, Germany

⁵Hubble Fellow, Institute for Astronomy, University of Hawaii, 2680 Woodlawn Drive, Manoa, HI 96822

⁶Space Telescope Science Institute, 3700 San Martin Drive, Baltimore, MD 21218

⁷Laboratory for High Energy Astrophysics, NASA/GSFC, code 662, Greenbelt, MD 20771

⁸Department of Astronomy, Leiden Observatory, P. O. Box 9513, 2300 RA, Leiden, The Netherlands

1. Introduction

The 1 Ms exposure of *Chandra* Deep Field South (CDFS, e.g. Giacconi et al. 2002; Rosati et al. 2002), along with the 2 Ms exposure of *Chandra* Deep Field North (CDF-N, e.g. Brandt et al. 2001; Alexander et al. 2003) are the deepest X-ray image ever taken. With these two deep surveys, the cosmic X-ray background discovered by Giacconi et al. (1962), the origin of which has been a major goal of X-ray astronomy for almost four decades, is now almost completely resolved into individual sources. Most of these X-ray sources are extragalactic, harboring supermassive black holes. The major goal now is studying the properties of these X-ray sources and understanding their physical nature.

Most recent *Chandra* and *XMM* observations have detected relativistic outflows with bulk velocity of $v_{\text{out}} \sim 0.6 - 0.7c$ in several active galactic nuclei (Yaqoob et al. 1998, 1999; Wang et al. 2003), revealed by extremely blueshifted emission lines due to iron or other elements in the X-ray spectra. In this letter, we report the discovery of a strong and blueshifted X-ray absorption feature (suggesting an even higher $v_{\text{out}} \sim 0.7 - 0.8c$) in one of the CDF-S sources, CXO CDFS J033260.0-274748 (hereafter CDFS11).

2. The Data and X-ray spectral fitting

The 1 Ms *Chandra* exposure on CDF-S was composed of eleven individual ACIS observations obtained from October 1999 to December 2000. Giacconi et al. (2002) presented the detailed X-ray data reduction and the final X-ray catalog (see also Alexander et al. 2003). The source CDFS11, $\sim 7'$ from the center of the field, was observed in all the eleven exposures. Its X-ray radial intensity profile is consistent with that of a point-source (Giacconi et al. 2002), and no other X-ray source was detected within $45''$. The optical counterpart of CDFS11 ($R_{\text{vega}} = 21.8$) was selected using the deep optical image ($R_{\text{vega}} < 26$), obtained with the FORS1 camera on the ANTU telescope (UT-1 at VLT). Giacconi et al. (2002) presented the *R*-band image cut-out, overplotted with X-ray flux contours (see their Fig. 13r). We can clearly see a single point-like optical counterpart located right at the center of the X-ray contours, with no nearby optical source within $7''$. The source was firmly classified as a quasar at $z = 2.579$ by the follow-up spectroscopy observations (see Fig. 6 of Szokoly et al. 2004). The X-ray to optical flux ratio $\log(f_{2-10\text{keV}}/f_R)$ is 0.3, typical for AGNs (see, e.g. Hornschemeier et al. 2001). A weak, flat-spectrum radio counterpart has also been detected with the VLA with flux densities of 36 ± 10 microJy at 6cm, and 33 ± 11 at 22cm (Kellermann et al. in preparation), making it radio quiet with radio-to-optical ratio $f_{1.4\text{GHz}}/f_R \sim 6$.

We extract the *Chandra* ACIS-I X-ray spectrum of CDFS11 from a circle with radius of

7", which is the 95% encircled-energy radius of the ACIS point-spread function at the source position. The local background was extracted from an annulus with outer radius of 19" and inner radius of 9". In Fig. 1 we present the summed spectrum (source plus background) and the background evaluated in the outer annulus. The source is fairly bright in X-ray with ~ 1040 net X-ray counts in the 0.5 – 2.0 keV band and ~ 350 in the 2.0 – 9.0 keV band, allowing us to perform X-ray spectroscopy. During the fit, we use the C statistics (Cash 1979; Nousek & Shue 1989), which has better performance with respect to the χ^2 analysis, particularly for spectra with low detected counts. We generate the X-ray telescope response and ACIS-I instrument response for each single *Chandra* observation, and sum the response files weighting them for the corresponding exposure times. The final time-weighted response files were used for spectral analysis. We utilize XSPEC v11.2 to perform the spectral fitting. All the spectral fitting was done in the energy band 0.5 – 9.0 keV and all the statistical errors quoted in this paper are at the 90% confidence level for one interesting parameter.

We first fitted the spectrum with a simple power-law plus a neutral absorber in the source frame. A Galactic neutral hydrogen absorption column of $8 \times 10^{19} \text{ cm}^{-2}$ (Dickey & Lockman 1990) was also included. The results are presented in Table 1. The spectrum was well fitted by a power-law ($\Gamma = 1.7_{-0.1}^{+0.1}$) with weak absorption ($N_H = 0.1_{-0.1}^{+1.0} \times 10^{22} \text{ cm}^{-2}$). The intrinsic, rest-frame 2.0 – 10.0 keV luminosity is $4.3 \times 10^{44} \text{ ergs s}^{-1}$ ($H_0 = 70.0 \text{ km s}^{-1} \text{ Mpc}^{-1}$, $\Omega_m = 0.27$, $\Omega_\Lambda = 0.73$). The best-fit continuum model and the ratio of data to model is shown in Fig. 2. Both in Fig 1 and 2, we can see a strong absorption feature at $\sim 6.3 \text{ keV}$ in the observed frame. The absorption appears to be optically thick, since the ratio of data to model reaches zero at energies around 6.3 keV.

We add an absorption edge to our fit, which attenuates the continuum above E_{edge} with the optical depth $\tau = \tau_0(E/E_{edge})^{-3}$. An absorption edge with $E_{edge} = 5.8 \text{ keV}$ and $\tau_0 = 3.5$ significantly improves the fit ($\Delta C = -15$ with two extra free parameters, see Table 1). We also tried to model the absorption feature by a saturated absorption line model. The model *notch* of XSPEC was used by fixing the covering fraction at 0.99 to represent a blank absorption trough. The fitting is slightly better than the edge model with $\Delta C = -17$ for two extra free parameters, which are located at $E_c = 6.3 \text{ keV}$, and the line width of 0.9 keV (both in the observed frame). The line width can also be taken as the equivalent width of the absorption line since the absorption is saturated. We also perform spectral fits to search for possible other absorption edges/lines at lower energies. We try different energy entries from 0.5 to 6 keV, but we find that no further absorption edge/line is statistically required ($\Delta C < 3$).

The X-ray spectrum of CDFS11 was found to be variable with high probability ($> 3\sigma$, Paolillo et al. 2004). However, due to the limited number of X-ray photons over 5 keV,

and the fact that the absorption feature is optically thick with black trough, we are unable to study the variability of the absorption itself, based on our data. Sometimes, a broad emission line might actually be mimicked by a strong absorption edge at higher energy (e.g., Reeves, Porquet & Turner 2004) and vice versa, especially in X-ray spectra with low S/N or low energy resolution. To check if this is the case for CDFS11, we fit the spectrum with a power law continuum and a broad emission line. We tried different central values for the line energy from 4 to 6 keV, and found that an emission line can only improve the C statistics by $\Delta C \leq -2$. This indicates that the absorption feature in CDFS11 can't be ascribed to the presence of a broad emission line.

3. Discussion

We discuss here the possible origin of the significant broad absorption feature we detected in the X-ray spectrum of CDFS11 with the 1Ms *Chandra* ACIS exposure. The feature locates at energies > 20 keV in the rest frame, with a confidence level of 99.98% according to F-test. We note that the confidence level given by F-test for an absorption feature might not be accurate (Protassov et al. 2002). Here we re-estimate the confidence level of the absorption feature via a simple approach. In the energy range 5.8 – 6.8 keV where the absorption feature is located, we detected a total of 11 photons (source + background), while the continuum model plus background predict 32 photons. The cumulative Poisson probability for such a deviation is $\sim 1.7 \times 10^{-5}$. Since the absorption feature was examined over the whole spectral band, which is 0.5 – 9.0 keV, the probability of detecting such a broad spurious absorption feature randomly in the spectrum is approximately $1.7 \times 10^{-5}/(9.0 - 0.5) = 2.0 \times 10^{-4}$. This is consistent with the confidence level obtained with the F-test.

We also perform extensive Monte Carlo simulations to check the confidence level. First, we simulate 10^4 artificial spectra based on the best-fitting continuum model. We then search for spurious absorption lines in the artificial spectra by adding a notch component. All the three parameters of the notch model (central energy, width, and covering factor) are thawed. We did not fix the covering factor at 0.99 during the simulation because shallower absorption line (i.e., with lower covering factor) can reach comparable significance level at lower energy due to the higher S/N. To ensure an efficient search over the whole band, we perform the search in narrow energy bins (such as 0.5–1.5 keV, 1.5–2.5 keV, etc) with width comparable to that of the observed absorption feature, and count the total number of spectra in which we detected spurious absorption line with $\Delta C < -17$. We found only 6 spectra with statistically significant broad (energy width > 0.5 keV) spurious absorption lines. This

indicates a confidence level of 99.94% for the broad absorption feature we detected. Note also that, while fitting the real spectra, we use only 2 free parameters of the notch model, while in the simulation, we use 3. We remark that the confidence level would be higher (99.98%) if we searched for spurious features with $\Delta C < -19.6$ for 3 free parameters, instead of $\Delta C < -17$ for 2.

We note that there is also weak evidence of the absorption feature in the 370 ks XMM spectrum (Streblyanska et al. 2004) of CDFS11. The XMM spectrum is significantly steeper ($\Gamma = 2.3$) and it was obtained about one year later. The statistical quality of the XMM spectrum around 6 keV is much lower due to the high background noise and the steeper continuum. By fitting the Chandra and XMM spectra simultaneously, we found an even higher confidence level of 99.997% for the absorption feature, based on F-test. However, due to the very limited statistical quality, we are unable to use the XMM spectrum independently to constrain the nature and possible time variability of the absorption feature.

We conclude that the confidence level of the absorption line we detected in CDFS11 is $> 99.98\%$. Even considering the number of all the CDFS spectra we examined for interesting features (~ 30 CDFS spectra have X-ray photons > 500 , whose quality is high enough to enable the search for broad line features), the absorption feature is still significant with a confidence level of 99.4%.

3.1. Instrumental Artifact?

Could such an unusual X-ray feature be due to any instrumental artifact or to some aspect of our analysis? We first consider improper background subtraction as a possible origin of the absorption feature. We check that we obtain consistent results when using background spectra extracted from different regions of the detector. We also note that the absorption feature is already significant in the spectrum *without* background subtraction. Finally, we do not see any bump at ~ 6 keV in the background spectrum either, suggesting that the significance level of the feature is not magnified by background subtraction. Therefore, we conclude that the absorption feature is not related to uncertainties in the background subtraction.

Could the absorption feature be an artifact of calibration uncertainty in the ACIS instrumental response function? As far as we know, no such an artifact (i.e., an absorption feature at ~ 6.3 keV) has been reported. We examined the spectra of nearby X-ray sources, but we found no evidence of absorption feature at ~ 6.3 keV among them. Tozzi et al. (2005) presented the X-ray spectra of CDFS sources using updated *Chandra* calibration files (with

CIAO3.0.1 and CALDB2.26 instead of CIAO2.0.1 and CALDB2.0 adopted in Giacconi et al. 2002 and in this letter). We repeated the fitting using the updated spectrum and obtained consistent results for both the continuum and the absorption feature. This confirms that the absorption feature is not due to improper data calibration. Note that Wang et al. (2003) reported a puzzling strong emission line at ~ 6.3 keV in the observed frame in CXO CDFS J033225.3-274219 (CDFS46). The two unusual features (the emission feature in CDFS46, and the absorption feature in CDFS11 reported in this letter) located at similar energies in the observing frame, could suggest a common origin related to instrumental effects. However, there are strong evidences against this occurrence: since the total exposure was composed of eleven individual observations with different roll angles, photons from each source fall into different positions on different chips during different observations. It is unlikely that an unknown instrumental artifact (if there is any) would affect photons from all eleven exposures. Furthermore, the two sources are around $9'$ apart, and fall into different chips during the observations. We conclude that the similar energy of the two features is just a coincidence.

3.2. The nature of the absorber

Among the heavy elements, iron is the only one that can produce such a strong absorption feature at high energies. However, the rest-frame energy of the absorption (> 20 keV) is too high for static iron in the rest frame, since the highest energy transition is the K-shell edge of H-like ion at 9.28 keV. Therefore we consider two possibilities: either the absorber locates at much lower redshift along the line of sight, or in an relativistic outflow intrinsic to the quasar.

The continuum fitting yields a marginal intrinsic absorption with $N_H \sim 10^{21}$ cm $^{-2}$, which is too small to account for the strong absorption feature at ~ 6.3 keV. We can't locate other absorption features either in the spectrum at lower energy (due to relatively lower ionized ions, such as the OVIII absorption edge at 0.87 keV). This suggests that the absorber has to be extremely ionized, with almost all abundant elements fully ionized, and the absorption is dominated by H or He-like iron atoms. Adopting the photon ionization absorption model *absori* (Magdziarz & Zdziarski 1995) to fit the spectrum, we obtain an ionization parameter¹ $\xi > 9000$ and $N_H > 3 \times 10^{24}$ cm $^{-2}$ (Table 1). Note the upper limits of ξ and N_H are poorly constrained since the two parameters are degenerate. Assuming $\xi = 10000$, we obtain $N_H = 5 \times 10^{24}$ cm $^{-2}$. We assume a temperature of 10^6 K and

¹ $\xi = L/nR^2$, where L is the integrated incident luminosity between 5 eV and 300 keV, n is the density of the material and R is the distance of the material from the illuminating source (Done et al. 1992).

solar abundance for the absorber. We note that an intrinsic absorption at the level of $N_H = 5 \times 10^{24} \text{ cm}^{-2}$ (well within the Compton-thick regime) would strongly attenuate the continuum photons. However, if the iron in the absorber is a factor of 10 overabundant with respect to the solar value, we obtain $N_H \sim 5 \times 10^{23} \text{ cm}^{-2}$.

The absorption feature can also be fitted by a broad saturated absorption line. The most likely responsible lines are 6.70 Fe_{XXV} K α (6.70 keV) and/or Fe_{XXVI} K α (6.97 keV). Assuming an average depth of the absorption line $\tau = 2$, and a factor of 10 overabundant for iron, we obtain $N_H \sim 5 \times 10^{23} \text{ cm}^{-2}$. We point out that for such an absorber, we also expect Fe_{XXV} K β (7.85 keV), Fe_{XXVI} K β (8.26 keV) absorption lines, and strong Fe_{XXV} (8.83 keV), Fe_{XXVI} (9.28 keV) absorption edges. Given the few counts we measure above 7 keV, we can't check the existence of these features. Future X-ray missions with higher sensitivity can help us to unveil the nature of the absorber by showing us the spectral properties at energies $> 7 \text{ keV}$ and the absorption profile with higher S/N.

If the absorption is due to foreground absorber, the absorber has to be located at a much lower redshift ~ 0.5 (if due to H or He-like iron absorption edges) or ~ 0.1 (if due to H or He-like iron resonant absorption line). The absorber must be extremely ionized with $N_H > 5 \times 10^{23} \text{ cm}^{-2}$. Note the foreground absorber is unlikely photo-ionized, otherwise we should have seen the extra photon ionization source, thus it has to be extremely hot with a temperature of $\sim 10^8 \text{ K}$ to reach the required ionization stage. Such a high temperature and N_H is very unusual for intervening systems. The only possible candidate is the hot intra-cluster medium found in clusters of galaxies (see Rosati, Borgani & Norman 2002 and references therein). However, for a cluster with $T = 10^8 \text{ K}$, we expect an X-ray luminosity of $\sim 3 \times 10^{45} \text{ erg s}^{-1}$ (based on the $L_X - T$ relation, e.g. Lumb et al. 2004). If located at $z \sim 0.5$, such a cluster would be around 300 times brighter than CDFS11, and its emission would be obviously prominent in the *Chandra* image. We conclude that the X-ray absorption feature we detected in CDFS11 can't be due to an intervening systems along the line of sight.

Finally, we consider a relativistic outflow intrinsic to the quasar, with speed of $\sim 0.7c$ (Doppler Factor $DF = 2.3$ for absorption edge) or $\sim 0.83c$ ($DF = 3.2$ for absorption line), to produce the observed blueshift of the absorption feature. Note that similar blueshifted features have been reported in the X-ray spectra of 3 AGNs: a highly blueshifted O_{VII} emission line in PKS 0637-75 with $DF \sim 2.7 - 2.8$ (Yaqoob et al. 1998); a blueshifted Fe-K emission line ($DF \sim 2.4 - 2.6$) in QSO PKS 2149-306 (Yaqoob et al. 1999); and a strong blueshifted Fe-K emission line ($DF \sim 2.3 - 2.5$) in CXO CDFS J033225.3-274219 (Wang et al. 2003). The good agreements of the blueshift factors from different sources strongly suggest a close origin of the relativistic outflow, and strengthen the statistical significance of these features.

Taking $\log \xi = 4$ and $N_H = 5 \times 10^{23} \text{ cm}^{-2}$, we estimate the distance of the absorber from the central source R by assuming the thickness of the absorber $\Delta R \sim 0.1R$. We obtain $R \sim 6 \times 10^{16} \text{ cm}$. Following Reeves, O’Brien & Ward (2003), we estimate the rate of relativistic outflow. The outflow rate (\dot{M}_{out}) can be calculated as $\dot{M}_{\text{out}} = \Omega v_{\text{out}} m_p L_X / \xi$. Assuming that the outflow subtends a solid angle of 0.1 steradian, we obtain a outflow rate of $\sim 10^{27} \text{ g s}^{-1}$ or $\sim 10 M_\odot \text{ year}^{-1}$, similar to that of the outflow in PDS 456 ($v_{\text{out}} \sim 0.17c$, Reeves et al. 2003). However, because of the extremely high outflow speed in this case, the kinetic energy carried by the relativistic material outflow would be $\sim 20 M_\odot \text{ year}^{-1}$, and then requires an accretion rate of at least $200 M_\odot \text{ year}^{-1}$ with an assumed energy production efficiency $\epsilon = 0.1$ which entirely goes into the outflow. Such an accretion rate is far beyond the Eddington limit even for a supermassive black hole of $10^8 M_\odot$ ($\sim 3 M_\odot \text{ year}^{-1}$). To keep the rate of kinetic energy outflow lower than that released by Eddington accretion, a more reasonable outflow rate would be at least 100 times smaller ($< 0.1 M_\odot \text{ year}^{-1}$), and so does the solid angle (< 0.001 steradian). The extremely high velocity and small covering factor strongly link the physics of the outflow to relativistic jets in AGN and X-ray binary systems (such as the famous XRB SS 433, see Migliari, Fender & Méndez 2002).

We conclude that the X-ray absorption feature in CDFS11 is due to an ionized jet-like outflow intrinsic to the quasar, with a bulk velocity of $\sim 0.7 - 0.8 c$. Similar outflows have been reported in the X-ray spectra of several other AGNs. Future X-ray mission with higher intensity can help us understand the nature of the outflows by providing X-ray spectra with higher S/N.

The work of JW was supported by Chinese NSF through NSF10473009 and the CAS ”Bai Ren” project at University of Science and Technology of China.

Table 1. Spectral fits to CDFS11

continuum	Γ	$N_H(10^{22}\text{cm}^{-2})$	C/dof
	$1.7_{-0.1}^{+0.1}$	$0.1_{-0.1}^{+1.0}$	362/356
edge	$E_{edge}(\text{keV})$	τ_0	C/dof
	$20.9_{-0.5}^{+0.7}$	$3.5_{-1.2}^{+...B}$	347/354
notch ^A	$E_c(\text{keV})$	Width(keV)	B/dof
	$22.5_{-0.3}^{+0.5}$	$3.0_{-1.1}^{+0.9}$	345/354
absori	ξ	$N_H(10^{22}\text{cm}^{-2})$	C/dof
	>9000	>500	344/353

^AThe covering factor of the notch model was fixed to 0.99 to represent a heavily saturated absorption.

^BThe upper limit of the absorption depth was poorly constrained.

REFERENCES

- Alexander, D. M., et al. 2003, AJ, 126, 539
- Brandt, W. N., et al. 2001, AJ, 122, 2810
- Cash, W. 1979, ApJ, 228, 939
- Dickey, L. M., & Lockman, F. J. 1990, ARA&A, 28, 215.
- Done, C., Mulchaey, J. S., Mushotzky, R. F., & Arnaud, K. A. 1992, ApJ, 395, 275
- Giacconi, R., Gurksy, H., Paolini, F.R., & Rossi, B.B., 1962, Phys. Rev. Letters, 9, 439
- Giacconi, R., et al. 2002, ApJS, 139, 369
- Hornschemeier, A. E., et al. 2001, ApJ, 551, 742
- Lumb, D. H. et al. 2004, A&A, 420, 853
- Magdziarz, P., & Zdziarski, A. A. 1995, MNRAS, 273, 837
- Migliari, S., Fender, R., & Méndez, M. 2002, Science, 297, 1673
- Nousek, J. A., & Shue, D. R. 1989, ApJ, 342, 1207
- Paolillo, M. et al. 2004, ApJ, 611, 93
- Protassov, R.; van Dyk, D. A., Connors, A., Kashyap, V. L., & Siemiginowska, A, 2002, ApJ, 571, 545
- Reeves, J. N., O’Brien, P. T., & Ward, M. J. 2003, ApJ, 593, L65
- Reeves, J. N., Porquet, D., & Turner, T. J. 2004, ApJ, 615, 150
- Rosati, P., et al. 2002, ApJ, 566, 667
- Rosati, P., Borgani, S., & Norman, C. 2002, ARA&A, 40, 539
- Streblyanska, A., Bergeron, J., Brunner, H., Finoguenov, A., Hasinger, G., Mainieri. V. 2004, *Nuc. Phys. B (Proc. Supp.)*, 132, 232
- Szokoly, G. P., et al. 2004, ApJS, 155, 271
- Tozzi, P, et al. 2005, A&A submitted
- Wang, J. X. et al. 2003, ApJ, 590, L87
- Yaqoob, T., George, I.M., Turner, T.J., Nandra, K., Ptak, A., & Serlemitsos, P.J. 1998, 505, L87
- Yaqoob, T., George, I.M., Nandra, K., Turner, T.J., Zobair, S., & Serlemitsos, P.J. 1999, ApJ, 525, L9

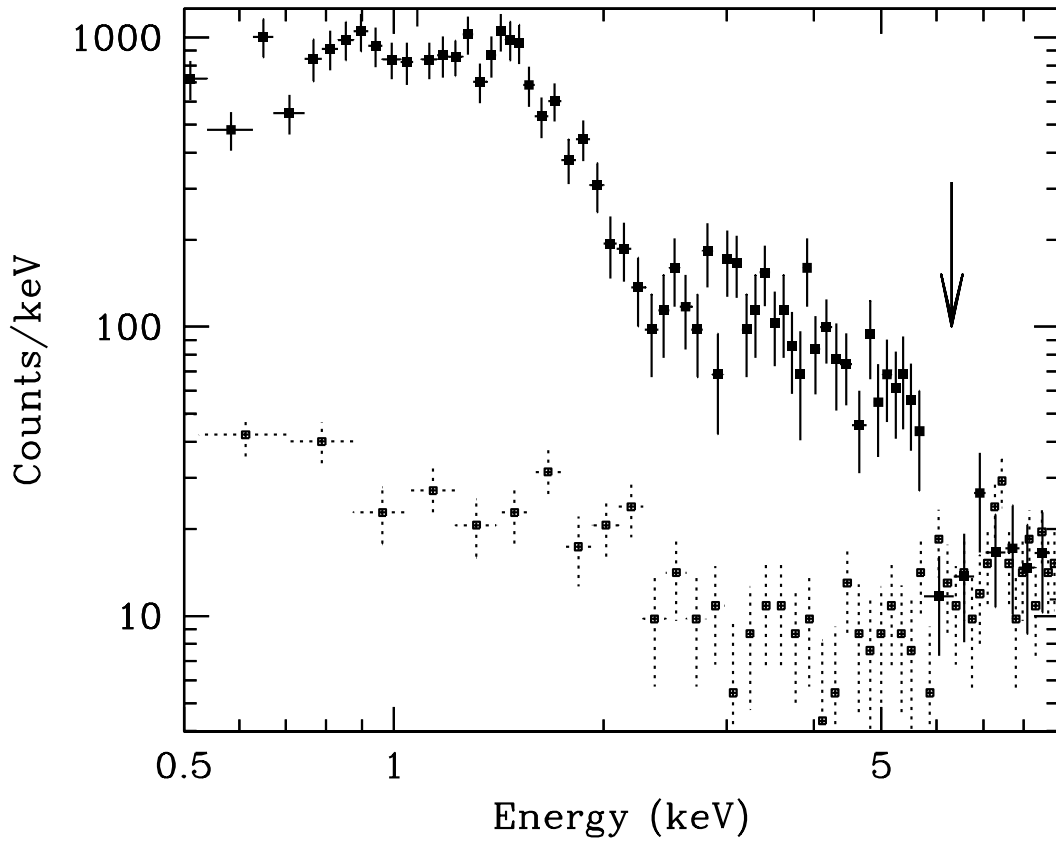


Fig. 1.— The summed (source plus background) X-ray spectrum of CDFS11 and the expected background (points with dotted error bars). The spectra were rebinned for display purpose.

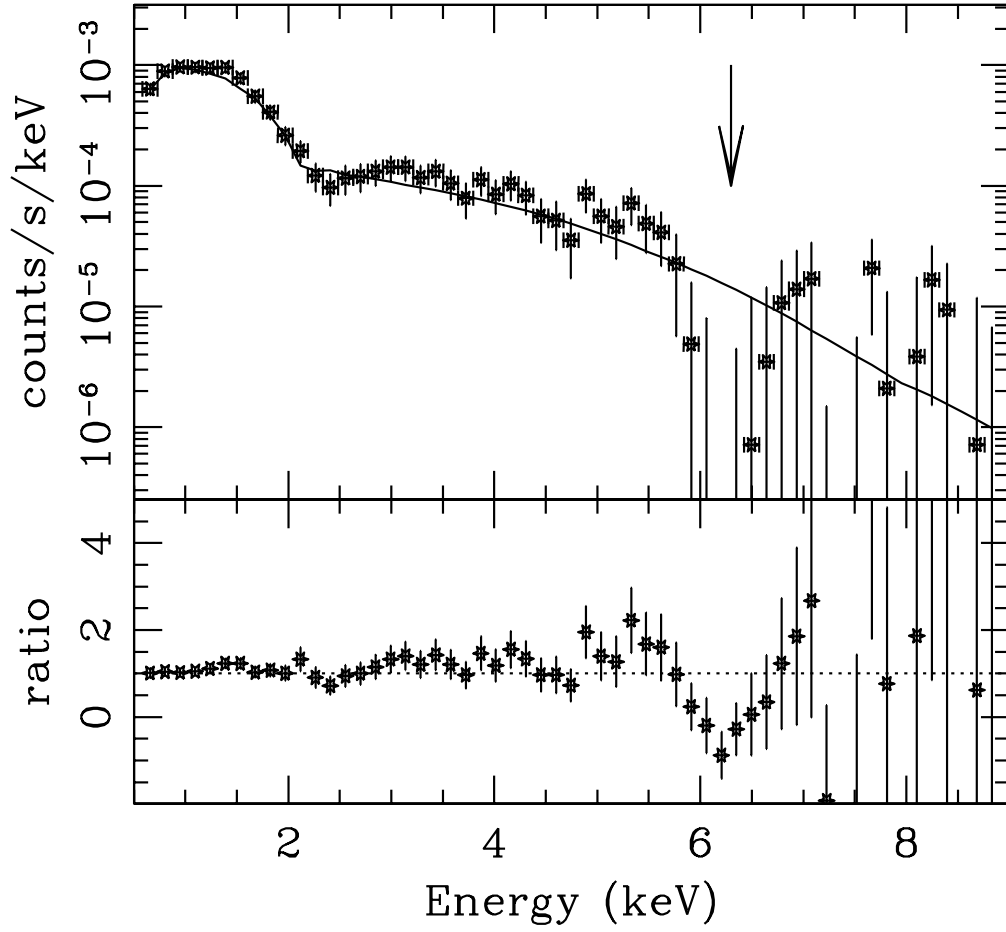


Fig. 2.— The spectral data (rebinned for display purpose), best-fit continuum models and the ratios of data to model for CDFS11.